As originally published in the IPC APEX EXPO Conference Proceedings.

A Control-Chart Based Method for Solder Joint Crack Detection

Jianbiao Pan
California Polytechnic State University, San Luis Obispo, CA 93407

Abstract

Many researchers have used different failure criteria in the published solder joint reliability studies. Since the reported time-to-failure would be different if different failure criteria were used, it would be difficult to compare the reported reliability life of solder joints from one study to another. The purpose of this study is to evaluate the effect of failure criteria on the reported thermal fatigue life and find out which failure criterion can detect failure sooner. First, the application of the control-chart based method in a thermal cycling reliability study is described. The reported time-to-failure data were then compared based on four different failure criteria: a control-chart based method, a 20% resistance increase from IPC-9701A, a resistance threshold of 500Ω, and an infinite resistance. Over 3.5 GB resistance data measured by data loggers from a low-silver solder joint reliability study were analyzed. The results show that estimated time-to-failure based on the control-chart method is very similar to that when the IPC-9701A failure criterion is used. Both methods detected failure much earlier than the failure criterion of a resistance threshold of 500Ω or an infinite resistance. A scientific explanation is made of why the 20% increase in IPC-9701A is a reasonable failure criterion and why the IPC-9701A and the control-chart based method produced similar results. Three different stages in resistance change were identified: stable, crack, and open. It is recommended that the control-chart based method be used as failure criterion because it not only monitors the average of resistance, but also monitors the dispersion of resistance in each thermal cycle over time.

Keywords: failure criterion, solder joint, interconnection, reliability, control chart

1. Introduction

One of the challenges in an experimental study of solder joint reliability is to determine when cracks occur in a solder joint. The most common way is through resistance measurement of a solder joint or a daisy chain. This method is based on the assumption that resistance will increase significantly or an electrical discontinuity will occur if there is a crack or cracks in a solder joint. The question is how to define a failure of a solder joint based on measured resistance value?

The current industry standards for solder joint failure criteria are IPC-9701A for thermal cycling testing, JESD22-B111 for drop testing, and IPC/JEDEC-9702 for bend testing. Note that IPC-9701A (released in 2006) is the latest revision of IPC-9701 (released in 2002), which replaces IPC-SM-785 (released in 1992). Failure definition for an event detector and a data logger is different. Table 1 lists the detailed failure criteria for each test. However, how the 1000 Ω, 100 Ω, and the 20% values were chosen is not documented.

Table 1. Current Industry's Failure Definition

Standard	Test	Failure definition	
		Event detector	Data logger
IPC-9701A (2006)	Temperature cycling & vibration	The 1st event of resistance exceeding 1000 Ω for lasting >1 μs, followed by >9 events within 10% of the cycles to initial failure	20% resistance increase in 5 consecutive readings
JESD22-B111 (2003)	Drop test	The 1st event of resistance > 1000 Ω for a period of >1μs, followed by 3 additional such events during 5 subsequent drops.	1st detection of resistance value of 100 Ω if initial resistance is <85 Ω, or 20% increase in resistance if initial resistance is >85 Ω, followed by 3 additional such events during 5 subsequent drops.
IPC/JEDEC-9702 (2004)	Bend test	20% resistance increase. A lower or higher threshold may be more appropriate, depending upon test equipment capability and specific daisy-chain design scheme.	

Because it is not clear how these values were chosen, many researchers have used different failure criteria in solder joint reliability studies. For example, the following failure criteria are used in the vibration test: a 10% increase in resistance (Kim et al. 2006), a 50% increase in daisy chain resistance (Che & Pang, 2009; Yang et al. 2000), a 100% increase in resistance (Wong et al. 2007), a resistance threshold of 50 Ω (Qi et al. 2007), and a resistance threshold of 100 Ω (Perkins and Sitaraman, 2008). The following failure criteria have been used in the thermal fatigue reliability test: an increase in resistance of 5 Ω (Suhling et al. 2004), an increase in resistance of 10 Ω (Farooq et al. 2003), a resistance threshold of 300 Ω (Che and Pang, 2013), and a resistance threshold of 450 Ω (Lau et al. 2004). It should also be noted that many reported studies used industry standards.

The reported time-to-failure would be different if different failure criteria were used. The question is how much difference. If the reported life were significantly different, it would be difficult to compare the reported reliability life of solder joints from one study to another since so many failure criteria are used. There are conflicting results. Henshall et al. (2009) evaluated the impact of three failure criteria, a 20% resistance increase, a resistance threshold of 500 Ω, and an infinite resistance (hard open). They found that the 20% resistance increase criterion gives typically 200 to 500 cycles less in characteristics life, or about 3% to 10% of lifetime, than the 500 Ω or hard open resistance criteria. But Xie et al. (2010) reported no significant difference in cycles-to-failure between the 20% resistance increase and over 1000 Ω (hard open) resistance criteria.

The reason why so many failure criteria are used is that it is still not well understood what is the relationship between the crack area of an interconnection and the change in resistance of the interconnection. When a crack is initiated in an interconnection, can it be detected by monitoring the change of resistance? One may believe that if a measurement system has enough precision, the change in resistance can be measured when a small crack occurs in the interconnection. Due to limited resolution of commercial multi-meters, researchers have developed the electrical resistance spectroscopy method for detecting early failures in solder joints under thermal fatigue reliability testing [Constable and Lizzul, 1995]. They used a lap shear test and measured the resistance change as a function of the applied strain. Lall, et al. [2009] extended this method for prognostication under shock and vibration reliability testing. Though both studies reported the success in detecting early failure, electrical resistance spectroscopy method has not been popularly used in the industry.

Pan and Silk (2011) proposed that the failure of an interconnection is defined as the resistance increase in a solder joint exceeding a threshold. Instead of setting the threshold as 20% above the initial resistance value, they used X-bar and R control charts to determine the threshold. In the drop and vibration tests, they defined the failure as the resistance increase by *k* times the range over the natural variation in resistance measured by a measurement system.

In this study, the application of the control-chart based method for solder joint failure detection in a thermal fatigue study is presented. The time-to-failure data based on this method are compared with the failure-to-failure data based on three other failure criteria, a 20% resistance increase, a resistance threshold of 500 Ω, and an infinite resistance (hard open). The 3.5 Gb resistance data measured by data loggers from a low-silver BGA thermal fatigue reliability study were analyzed. The purpose of this comparison is to evaluate the effect of failure criteria on the reported thermal fatigue life and find out which failure criterion can detect failure sooner. The behavior of resistance change will be analyzed as well.

2. Theoretical Background

Any measurement data include natural variability or "background noise." For example, the resistance change due to the change of temperature in a thermal fatigue reliability test is part of this natural variability. Figure 1 shows an example of resistance change of solder joints in a daisy-chain as the temperature change. Such variability in resistance is inherent because the resistivity of metals such as SnAgCu in solder joints and Au in wire bonds changes with temperature. In this case, about 1 Ω difference in resistance when the temperature changed from 0°C to 100 °C is observed. This variability due to thermal effect is a chance cause of variance, or natural variability. In additional, the natural variability also includes variation caused by the measurement system, such as gauge repeatability and reproducibility (GR&R). If the change of resistance is significant larger than the variability due to thermal effect and GR&R, it indicates that something else such as cracks initiated and propagated in a solder joint may play a role. The resistance change due to the cracks is an assignable cause of variation.

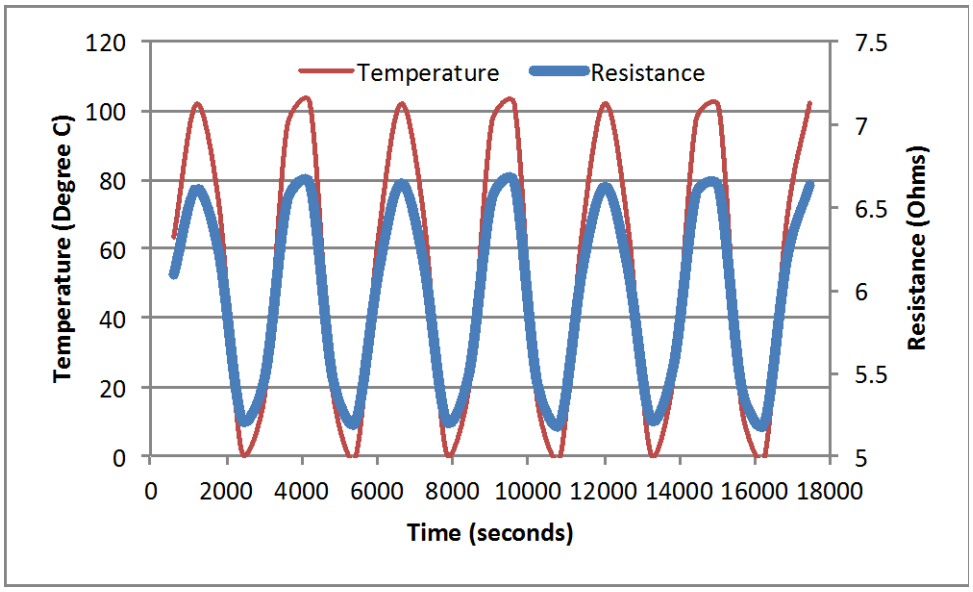

Figure 1. Resistance is a function of temperature.

The Shewhart control chart can be used to detect the assignable cause of variation from the chance cause of variation. The formulas for calculating control limits of X-bar and R charts are

Control limits for X-bar chart are $UCL_{\bar{X}} = \bar{\bar{X}} + \frac{k}{d_2\sqrt{n}}\bar{R}$ $LCL_{\bar{X}} = \bar{\bar{X}} - \frac{k}{d_2\sqrt{n}}\bar{R}$ (1)

Control limits for R chart are $UCL_R = (1 + k\frac{d_3}{d_2})\bar{R}$ $LCL_R = (1 - k\frac{d_3}{d_2})\bar{R}$ (2)

where $UCL_{\bar{X}}$ and $LCL_{\bar{X}}$ are upper control limit and lower control limit of the $\bar{X}$ chart, UCL_R and LCL_R are upper control limit and lower control limit of the R chart, $\bar{\bar{X}}$ is the average of the subgroup average, $\bar{R}$ is the average of the subgroup range, d_2 and d_3 are factors that vary with the sample size of the subgroup and can be found at quality control textbooks [Montgomery, 2013; Besterfield, 2009]. k is the number of standard deviation of the statistics such as $\bar{X}$ or R.
The common practice in process control is set *k* value of 3. To reduce the probability of false failure detection, the *k* value can be set a higher value such as 5 or 10.

To construct control charts, we need to decide the rational subgroup. Note that the variation within a rational subgroup must be only due to chance causes. Since the resistance change within a thermal cycle in an uncracked solder joint is a function of temperature as shown in Figure 1, which is a chance cause, it is reasonable to choose each thermal cycle as the rational subgroup. Thus, the control chart is used to detect variability from assignable causes by comparing the variation in resistance among subgroups (thermal cycles) with the variation within a subgroup (a thermal cycle). Note that variation among subgroups is used to evaluate long-term stability of the process.

Next we need to determine the size of the sample or subgroup. The sample size affects the sensitivity of detecting process shift. In the low-silver BGA project [Henshall et al., 2009, 2010, 2011], there are 5 to 6 measurements in each thermal cycle. Because the sample size varies in different thermal cycles, the control limits varies as well. To make analysis simple, we use the larger control limits. The control limits are established based on the first 40 cycles if the data of the first 40 cycles were in control.

The Xbar chart monitors average resistance in a cycle over time, in which the thermal effect is removed. Any resistance increase in the Xbar chart would be due to assignable causes such as cracks. The R chart monitors the variability of resistance in a cycle over time. If the range of resistance in the R chart increases, it indicates that the interconnection is not stable, and thus, the integrity of solder joints is questionable.

An example of control charts for one daisy-chain is shown in Figure 2. It shows that the mean of resistance exceeds the upper control limit at Cycle 3494 and continues to increase after that. The range of resistance increases exceeds its upper control limit at Cycle 3495. The range of resistance in Cycle 3500 reaches over 400.

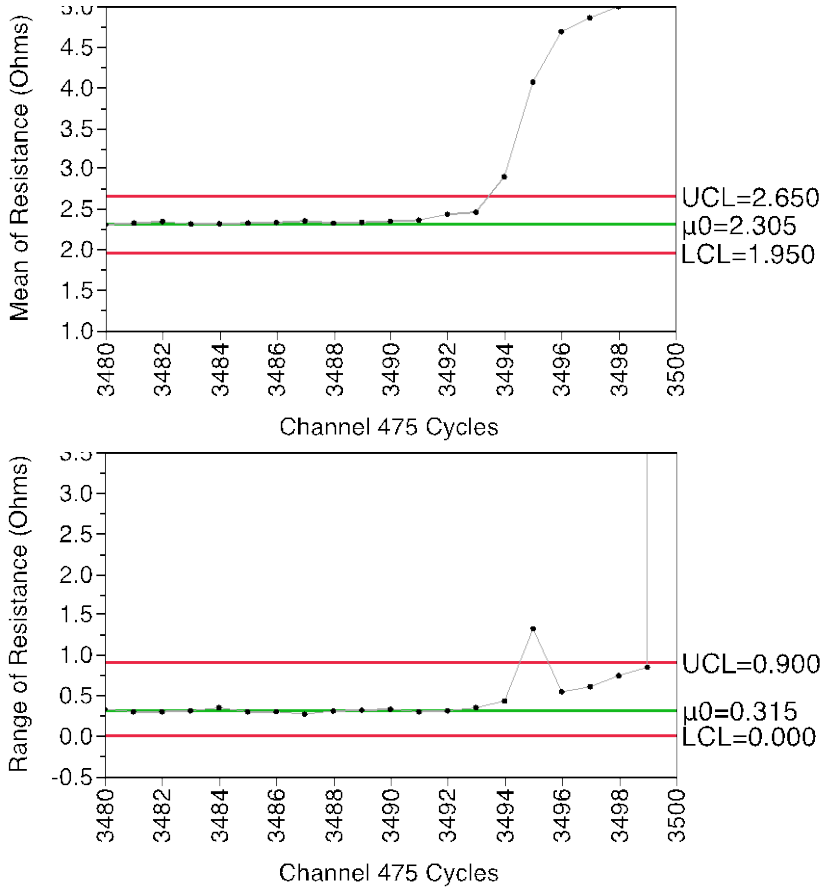

Figure 2. An example of control charts for one daisy-chain, Xbar chart (top), R chart (bottom)

3. Results

3.1 Effect of failure criteria on the reported thermal fatigue life

To investigate the impact of failure criteria on the reported thermal fatigue life, over 3.5 GB resistance data measured by data loggers from the low-silver BGA project [Henshall et al., 2010, 2011] were analyzed. The cycles-to-failure data for 1,440 daisy-chains were calculated based on four different failure criteria: the control-chart method, a 20% resistance increase from IPC-9701A, a resistance threshold of 500 Ω, and infinite resistance. Note that a resistance threshold of 500 Ω and infinite resistance failure criteria are used for comparison only. The failure definition of these four failure criteria were:

- The control-chart method: the first cycle of resistance exceeding the upper control limits of either the Xbar chart or the R chart.
- IPC-9701A: the first cycle of resistance exceeding 120% of the initial resistance value (or a 20% increase) at high temperature such as 100°C or 125°C. No consecutive readings were considered.
- Resistance threshold of 500 Ω: the first cycle of resistance reading greater than 500 Ω. No consecutive readings were considered.
- Infinite resistance: the first cycle of resistance reading reaches 9.90E+37 or the limit of a data logger. No consecutive readings were considered.

As an example, Figure 3 shows that the control-chart based method detected failure at Cycle 1,811, which is 18 cycles earlier than Cycle 1,829 detected by the IPC-9701A failure criterion. Figure 4 shows that the control-chart based reported failure of a daisy-chain at Cycle 6,366, while the IPC-9701A failure criterion reported failure at Cycle 6397, and the resistance threshold of 500 Ω failure criterion reported failure at Cycle 6,404. However, no failure is reported by the infinite resistance criterion because resistance has not reached the limit of the data logger when the test was terminated at Cycle 10,102.

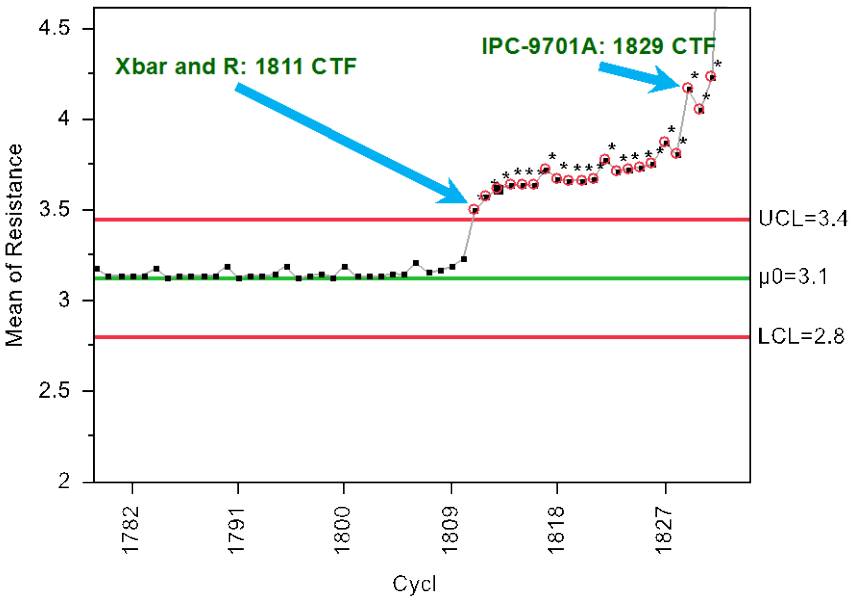

Figure 3. Comparison of cycles-to-failure between the control-chart based method and IPC 9701A for one daisy-chain.

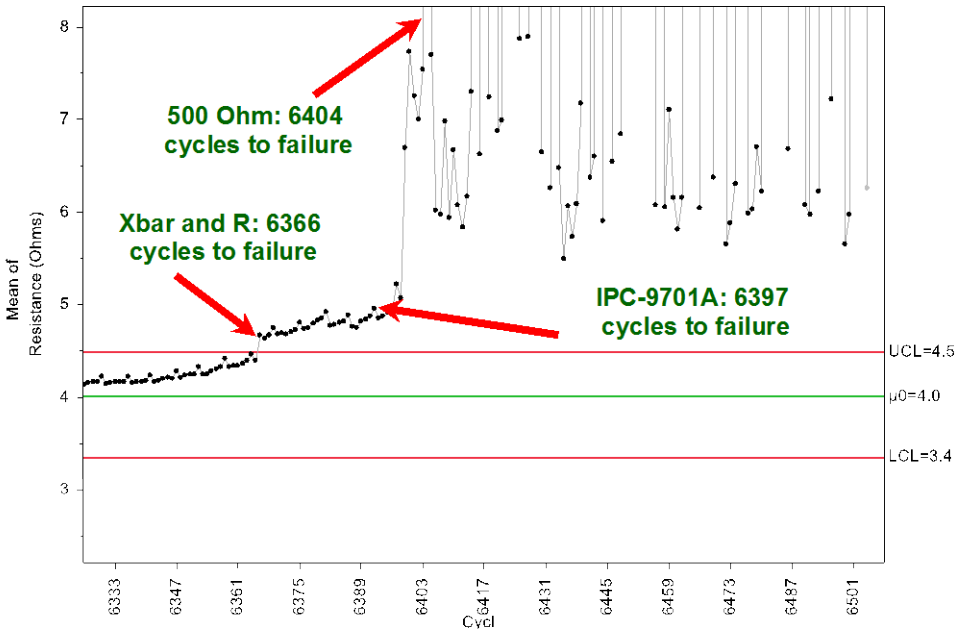

Figure 4. Comparison of cycles-to-failure between the control-chart based method, IPC 9701A, and the 500 Ω resistance threshold for one daisy-chain.

To understand the differences in reported thermal fatigue life among these failure criteria, paired tests have been conducted between IPC9701A and the control-chart based method, between the 500 Ω resistance threshold and the control-chart based method, and between the infinite resistance failure criterion and the control-chart based method. In the thermal cycle data from 0 to 100°C, there are 678 samples for analysis after excluding right-censored data (no failure). There are 710 samples for analysis for the thermal cycle data from -40 to 125°C.

Figure 5 shows a dot plot of the difference in the reported umber of cycles-to-failure between different failure criteria for the thermal cycle from the 0 to 100°C reliability test. The test statistics indicates that the control-chart based method failure criterion detected failure slightly sooner than IPC-9701A, with a mean in difference of cycles-to-failure of 2.83 cycles. Though 95% confidence interval of the mean between the IPC 9701A and the control-chart based method was between 1.91 and 3.75, the maximum difference was up to 176 cycles. The mean cycles-to-failure detected by the control-chart based method was 356 cycles earlier than the 500 Ω resistance threshold. The 95% confidence interval of the mean cycles-to-failure

between the 500 Ω resistance threshold and the control-chart based method was between 329 and 384, and the maximum difference was 2,459 cycles. The control-chart based method detected 861 cycles earlier in average with 95% confidence interval between 778 and 944 cycles than the infinite resistance failure criterion, and the maximum difference was up to 6,637 cycles. It is clear that the control-chart based method and IPC-9701A failure criteria are more sensitive than the 500 Ω resistance threshold and the infinite resistance failure criteria.

Figure 6 shows a dot plot of the difference in the number of cycles-to-failure between different failure criteria for the thermal cycle from -40 to 125°C reliability test. The test statistics indicates that there is almost no difference in the number of cycles-to-failure between the control-chart based method and IPC-9701A, with a mean of 0.85 cycles and 95% confidence interval of the mean between 0.53 and 1.18. Over 60% cases, the IPC-9701A and the control-chart based method reported the same number of cycles-to-failure. The mean cycles-to-failure detected by the control-chart based method is 97 cycles earlier than the 500 Ω resistance threshold and the maximum difference in reported cycles-to-failure was 1,396 cycles. The control-chart based method detected 231 cycles earlier in average than the infinite resistance failure criterion and the maximum difference in reported cycles-to-failure was 2,065 cycles.

Both Figures 5 and 6 show that the difference of the reported cycles-to-failure between the 500 Ω threshold or infinite resistance and the Xbar failure criteria are skewed to the right. Thus, the reported cycles-to-failure data based on the 500 Ω threshold or infinite resistance vary significantly, some even over 6000 cycles later than the Xbar or IPC9701A method in the thermal cycle from 0 to 100°C reliability test. This observation indicates that the slope in Weibull plot would be flatter when the 500 Ω threshold or infinite resistance failure criterion is used.

The above results indicate that the impact of failure criteria on the reported cycles-to-failure depends on the test conditions. The difference in the reported cycles-to-failure among different failure criteria is smaller at more severe conditions like thermal cycling from -40 to 125°C than less severe conditions such as thermal cycling from 0 to 100°C.

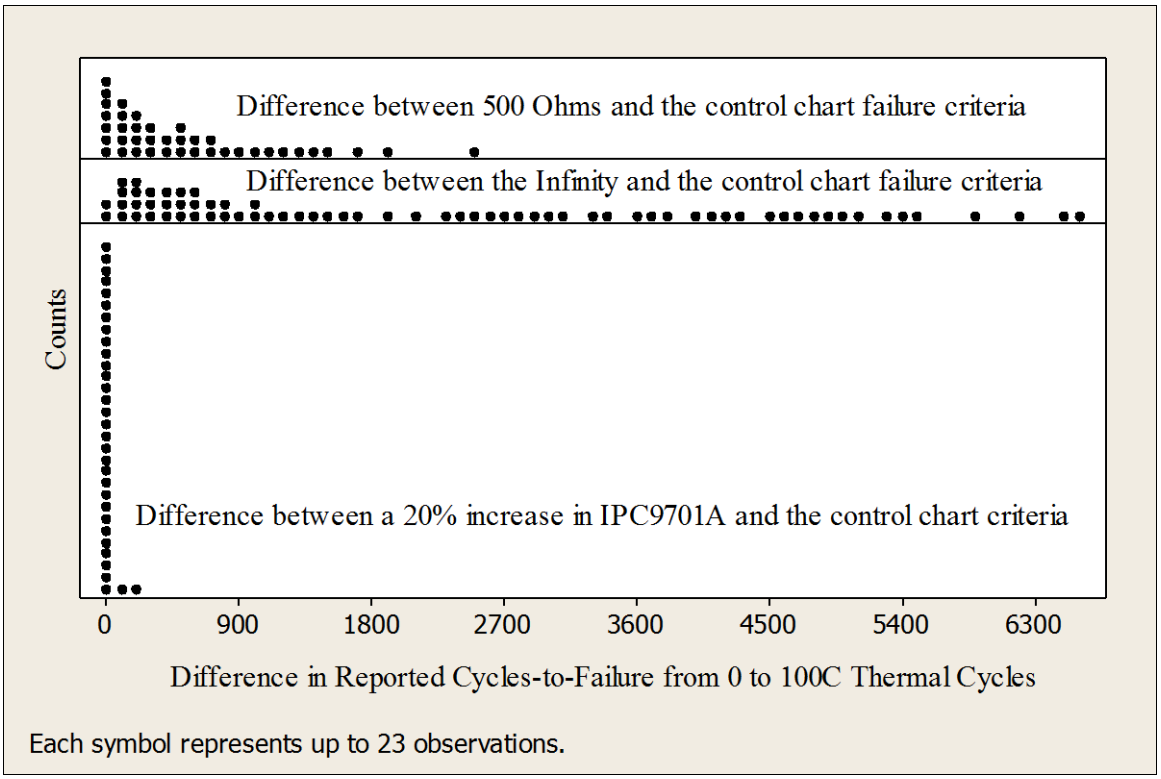

Figure 5. Dot plot of the difference in the number of cycles-to-failure between different failure criteria for the thermal cycle from 0 to 100°C reliability test (sample size of 678).

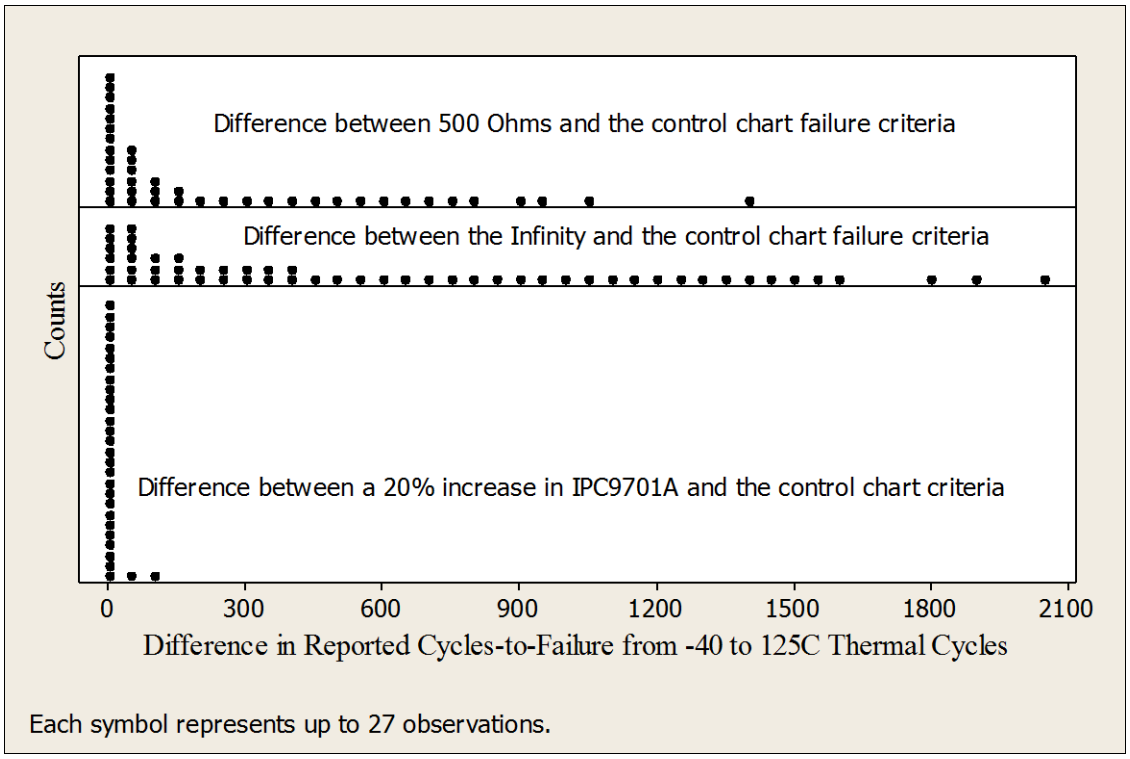

Figure 6. Dot plot of the difference in the number of cycles-to-failure between different failure criteria for the thermal cycle from -40 to 125°C reliability test (sample size of 710).

3.2 Characteristics of resistance change

To understand the above results on the effect of failure criteria on the reported thermal fatigue life, the resistance behavior was studied. Three stages of resistance behavior are identified: stable, crack, and open. An example of stable-crack-open is shown in Figure 7.

1) Stable stage. In this stage, both mean and range of resistance are in control. Before Cycle 3,555 in this example is the stable stage.
2) Crack stage. In this stage, mean and/or range of resistance exceed its upper control limit. Typically resistance has increased by more than 10% of initial resistance, but well below 100 Ω. As shown in Figure 7, the mean of resistance exceeds the upper control limit at around Cycle 3,560. The range of resistance increases as well, but may not reach its upper control limit. The increase in variability is a clear indication of cracks occurring in the solder joints. The crack stage could last several hundred cycles. In this example, the crack stage lasts 530 cycles from Cycle 3,560 to Cycle 4,090. From the stable stage to the crack stage, resistance could increase gradually as shown in Figure 8.
3) Open stage. In this stage, the resistance is over 1000 Ω. Examples are shown in Figure 7 (bottom) and Figure 9. During this period, resistance may flickeringly swing between very high resistance (over 1000 Ω to infinite) and just above the upper control limit for some time before it stays at infinite resistance. In this example, the flickering resistance (an on and off connection) lasts another 200 cycles.

In the stable stage, all these four failure criteria would report no failure. In the open stage, all failure criteria would detect failure. However, only the control-chart method and the IPC-9701A can detect failure in the crack stage in this example, while the 500 Ω resistance threshold and the infinite resistance failure criteria would report no failure because resistance is below their limit. Thus, the difference in the reported cycles-to-failure mainly depends on how long the crack stage is.

It is found that the duration of the crack stage depends on the severity of the test conditions. In severe test conditions like the -40°C to 125°C thermal cycling, the resistance behavior would often skip the crack stage or only have a few cycles during the crack stage. Figure 9 shows a case that resistance suddenly increases from the stable stage to the open stage. From resistance behavior of 80 daisy chains, it is found that the stable – crack – open trend occurred 95% of the time in the 0°C to 100°C thermal profile, a mild test condition, while the stable – open trend occurred 55% of the time in the -40°C to 125°C thermal profile, a severe test condition. Table 2 summarizes the results.

The small and gradual increase in resistance in a mild test condition suggested much later crack detection by the 500 Ω resistance threshold and the infinite resistance failure criteria. The characteristics of resistance behavior could explain the

difference in the reported cycles-to-failure among difference failure criteria. In a real application, loading is much lower than the accelerated test condition. Thus, resistance behavior of a real application is stable-crack-open and stays in the crack stage for a long time.

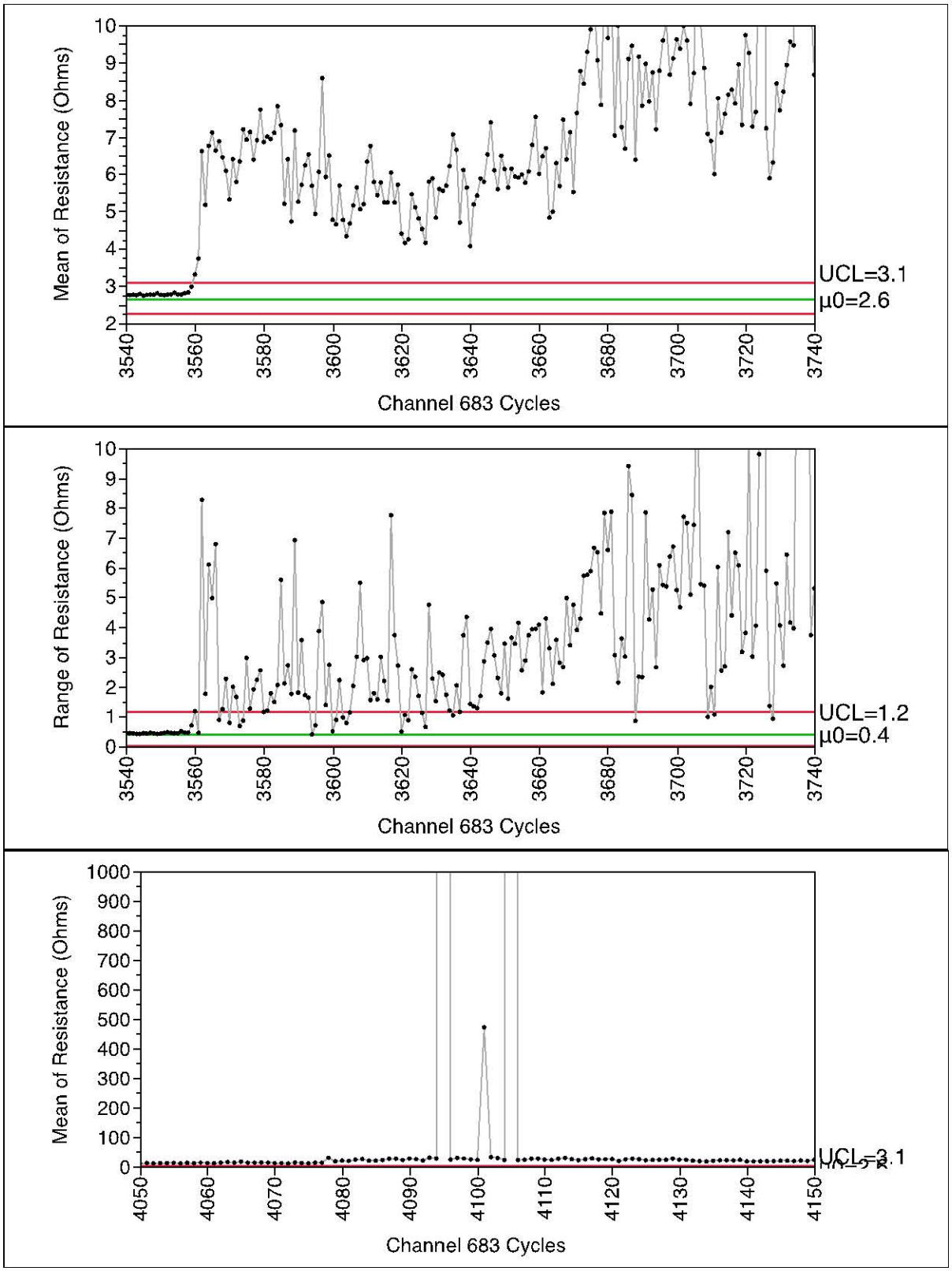

Figure 7. Resistance behavior of Channel 683, (top) mean of resistance from Cycle 3500 to Cycle 3700, (middle) range of resistance from Cycle 3500 to Cycle 3700, (bottom) mean of resistance from Cycle 4050 to Cycle 4150.

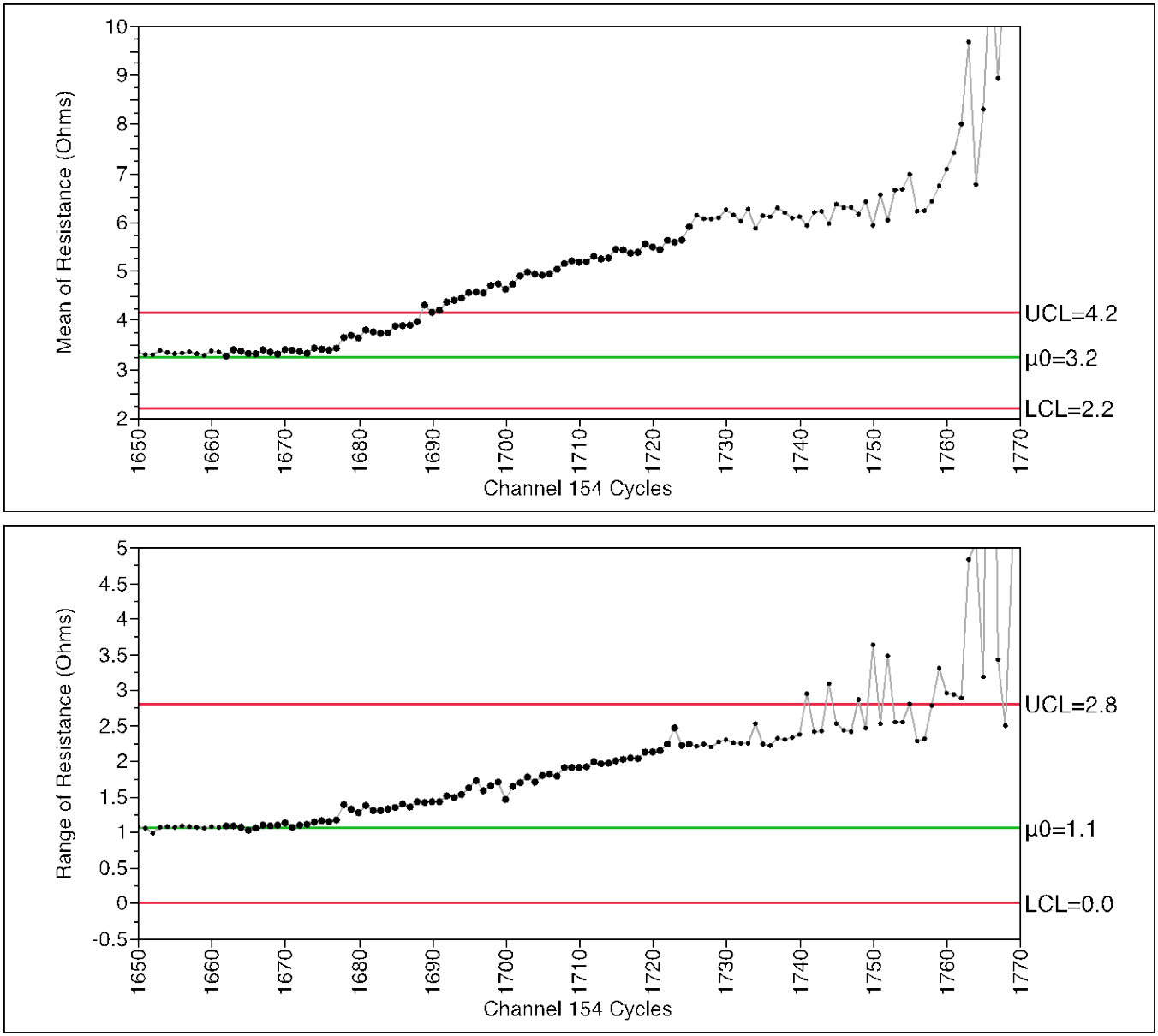

Figure 8. Resistance behavior of Channel 154, (top) mean of resistance from Cycle 1650 to Cycle 1770, (bottom) range of resistance from Cycle 1650 to Cycle 1770.

Table 2. Resistance behavior depending on the severity of test conditions

	Resistance pattern	
	Stable – Crack – Open	Stable - Open
Thermal cycling from 0 to 100°C	95%	5%
Thermal cycling from -40 to 125°C	45%	55%

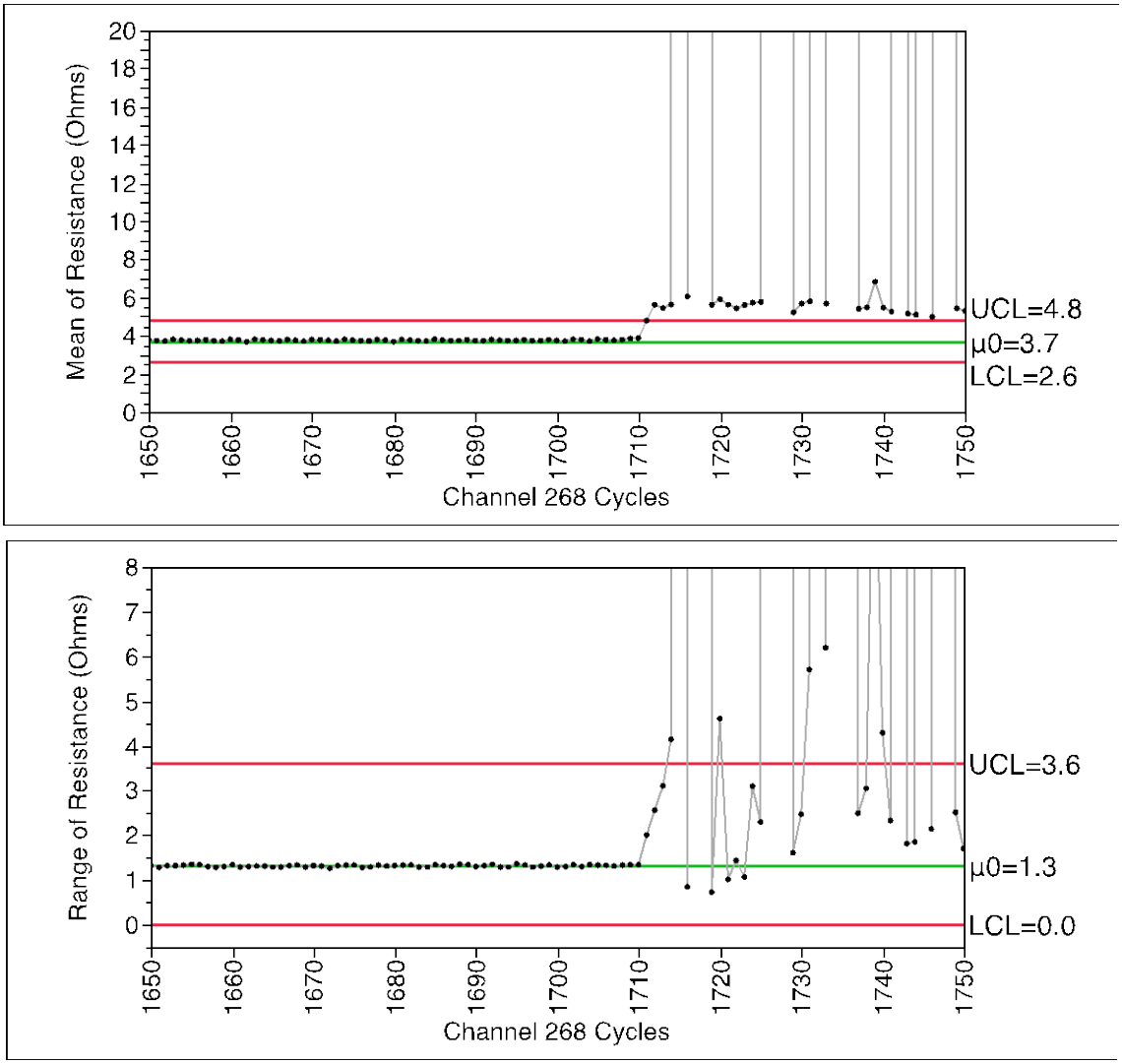

Figure 9. Resistance behavior of Channel 268, (top) mean of resistance from Cycle 1650 to Cycle 1750, (bottom) range of resistance from Cycle 1650 to Cycle 1750.

4. Discussion

4.1 The control-chart based failure criteria vs. a 20% increase in IPC-9701A

In the control-chart based method for solder joint failure detection, the failure of solder joints is defined as the resistance increase exceeding *k* times the natural variation. In thermal fatigue reliability tests, the natural variation is the variation in resistance due to temperature change.

Based on the physics of the temperature dependence of resistivity of metals such as gold (Au), tin (Sn), and copper (Cu), a change in resistance is proportional to the temperature change.

$$\Delta R = \alpha \Delta T R_0 \quad \text{or} \quad R(T) = R_0 + \alpha (T - T_0) R_0 \tag{3}$$

where ΔR is the change in resistance, α is temperature coefficient of resistance,

ΔT is the difference in temperature, R_0 is the resistance at temperature T_0

In a package with wire bonds, the resistance of a daisy-chain is mainly determined by the wire bonds, not the solder joints due to wire bonds' geometry of the long length and small diameter. Typical resistance value of a daisy-chain is a few ohms. The temperature coefficient of resistance of gold in wire bonds is about 0.0034/ºC.

Note in the flip chip case, the resistance of a daisy-chain is determined by the solder joints (SnAgCu), on-die wire resistance, and on-board wire resistance (Cu). Typical value is less than 1 Ω. The temperature coefficient of resistance of lead-free solder (SnAgCu) is about 0.0042/ºC and that of Cu is about 0.0039/ºC.

Figure 10 shows the relationship of the resistance and temperature for one daisy-chain having wire bonds inside the package. The data fits a linear regression line well as indicated by the coefficient of determination R^2 of 99%. The slope of 0.0143 Ω /ºC indicates that the resistance will increase by 0.0143 Ω when the temperature increases by 1 degree C.

From equation $\Delta R = \alpha \Delta T R_0$, we know theoretically the range of resistance purely due to thermal effect in the wire bonding case would be 34% (0.0034/ºC x 100ºC) of initial resistance at 0°C, or 29% (34%/(1+0.34/2)) of average resistance for the temperature cycling from 0 to 100°C. The range of resistance due to thermal effect would be 56% (0.0034/ºC x 165ºC) of initial resistance at -40°C, or 44% (56%/(1+0.56/2)) of average resistance for the temperature cycling from -40°C to 125°C.

The range of resistance is $\Delta R = \alpha \Delta T R_0 = \dfrac{\alpha \Delta T}{(1+\alpha \Delta T/2)} \bar{\bar{X}}$ where $\bar{\bar{X}}$ is the mean of resistance

The upper control limit of mean of resistance control chart is

$$\mathrm{UCL}_{\bar{R}} = \bar{\bar{X}} + \frac{k}{d_2\sqrt{n}}\Delta R = \bar{\bar{X}} + \frac{k}{d_2\sqrt{n}}\frac{\alpha \Delta T}{(1+\alpha \Delta T/2)}\bar{\bar{X}}$$

In this study, the sample size *n* is 5, so d_2 is 2.326. Given the temperature coefficient of resistance of 0.0034/ºC, the 3-sigma upper control limit of mean of resistance control chart is a 17% increase from the average resistance for the 0°C to 100°C thermal profile, and a 25% resistance increase from the average resistance for the -40°C to 125°C profile. This is why the reported cycles-to-failure data using the control-chart failure criterion is almost identical to that using a 20% increase failure criterion from the IPC-9701A. Note that we set the resistance threshold of IPC-971A as a 20% resistance increase from the resistance at *high temperature* such as at 100°C or 125°C. This analysis gives the number 20% in the IPC 9701A standard a scientific explanation.

4.2 Theoretical range of resistance purely due to thermal effects

Table 3 lists both theoretical and experimental values of range of resistance as a percentage of average resistance in a good solder joint due to thermal effects. Note that the theoretical range of resistance as a percentage of average resistance is calculated using equation $\dfrac{\alpha \Delta T}{1+\alpha \Delta T/2}$. One could conclude that an interconnection may have failed if the range is significantly larger than the theoretical range. The control-chart based method is able to monitor the dispersion in resistance for each thermal cycle over time.

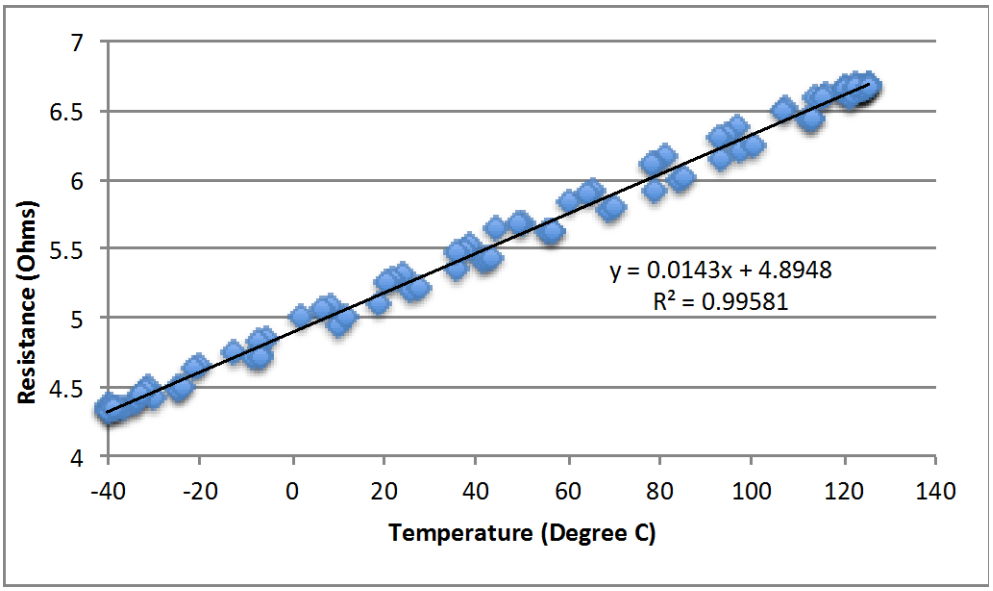

Figure 10. Resistance is a function of temperature

Table 3. Range of resistance due to thermal effects as a percentage of average resistance

Thermal profile range	Range of resistance as a percentage of average resistance			
	Wire bonding, $\alpha = 0.0034/°C$		Flip Chip, $\alpha = 0.0040/°C$	
	Theoretical value	Experimental data	Theoretical value	Experimental data
100°C (0°C to 100°C)	29%	25%*	33%	31%**
-40°C to 125°C	44%	43%*	50%	54%***
-55°C to 150°C	52%		58%	

* Data from the low-silver BGA project (Henshall et al. 2011)
** Data from Filho et al. 2006
*** Data from Stepniak, 2002

4.3 Relationship between the crack area and the resistance increase

To understand the relationship between the crack area of an interconnection and the change in resistance of the interconnection, a simple example is given. Assume the initial solder joint can be modeled as a simple cylinder with a diameter of 200 µm and a height of 120 µm. Given the electrical resistivity of Sn at 20ºC is about 1.09 x 10^{-7} Ωm, the resistance of the initial good solder joint is about 0.4 mΩ. Assume a crack occurs after the reliability testing and the cross-sectional area of the contact becomes a circle with a diameter of 20 µm and the gap of the crack is 1 µm. Thus, the increase in resistance due to the reduction of the contact area from the diameter of 200 µm to 20 µm will be

$$\Delta R = \rho\frac{l}{A_2} - \rho\frac{l}{A_1} = \rho\frac{4l}{\pi D_2^2} - \rho\frac{4l}{D_1^2} = 1.09\times10^{-7}\Omega m\times\frac{4\times1\mu m}{3.14\times(20\mu m)^2} - 1.09\times10^{-7}\Omega m\times\frac{4\times1\mu m}{3.14\times(200\mu m)^2} = 0.35 m\Omega$$

If the crack continues to increase and leaves the contact area as small as a cylinder with a diameter of 1 µm and a height of 1 µm, the increase in resistance will be just 0.14 Ω. When the contact area is only a cylinder with a diameter of 1 µm, a crack has propagated to become almost a full-crack.

Thus, in the stable stage where both mean and range of resistance are in control, cracks could have initiated and propagated but have not reached a full crack yet. In the crack stage where there is only a small increase in resistance (typically less than 1 Ω), at least one solder joint has propagated to almost a complete crack, or a full-crack has occurred but the failed solder joint was compressed by the surrounding good solder joints in a daisy-chain. Filho et al. (2006) verified the solder joint integrity after the first event that resistance increased from 32 mΩ to around 1 Ω and they observed a total-length crack in that solder joint after cross sectioning. Stepniak (2002) also observed heavily damaged solder joints with only small resistance increase. In the open stage, a complete crack has occurred and the gap of the crack is large.

4.4 Errors from different failure criteria

There are two types of errors that can occur in defining failure criterion. A Type I error is false detection, meaning an increase in resistance exceeds a threshold defined in a failure criterion but the truth is there is no crack in the solder joint. A Type II error is false pass, which happens when a crack occurs in the solder joint but the change in resistance does not reach the threshold defined in the failure criteria.

Using an event detector for failure detection can cause both errors. The event detector with high sampling rate is sensitive to electrical noise as acknowledged in IPC-9701. Qi et al. (2008) captured the resistance spikes due to noise using an oscilloscope. Thus, the event detector is prone to false detection, a Type I error. The resistance threshold of 1000 Ω defined in IPC-9701A for an event detector is too high to identify the crack stage, which leads to a false pass, a Type II error.

The author argues that the fixed resistance threshold such as 5 Ω, 450 Ω, or 1000 Ω is not a good failure criterion because the initial resistance value of a daisy-chain varies among different setups. For example, the initial resistance value could be from 32 mΩ in one study (Filho et al. 2006) to 15.74 Ω in another study (Wang et al., 1999). Since the theoretical range of resistance due to thermal effects is proportional to initial resistance, using percentage increase from the initial resistance as the failure criterion is recommended.

When resistance increase is small and gradual as shown in Figure 8, the cumulative sum control chart may detect failure earlier than traditional Shewhart control charts.

Conclusions

In this study, the application of the control-chart based method to detect solder joint failure in a thermal cycling reliability study is presented. In the control-chart based method, the thermal fatigue failure of solder joints is defined as the mean or range of resistance when the thermal cycle increases significantly, measured by *k* sigma of the natural variation purely due to thermal effects. Note that the variation from gauge repeatability and reproducibility is not considered here because it is typically much smaller than the variation due to thermal effects.

The reported cycles-to-failure data based on different failure criteria were compared. The results show that the reported cycles-to-failure from the control-chart method is very similar to that when the IPC-9701A failure criterion is used. Both IPC-9701A and the control-chart based method can detect failure much earlier than the failure criterion of a resistance threshold of 500 Ω or an infinite resistance.

A scientific explanation is made of why the 20% increase in IPC-9701A is a reasonable failure criterion and why the IPC-9701A and the control-chart based method produced similar results. From the physics of the metal's temperature dependence of resistance, the range of resistance purely due to thermal effects is calculated as the percentage of average resistance.

Three stages of resistance behavior are identified: stable, crack, and open. In the stable stage, cracks could have initiated and propagated but have not reached a full crack. In the crack stage where the increase in resistance is small (typically less than 1 Ω), at least one solder joint has propagated to almost a complete crack, or a full-crack has occurred but the failed solder joint was compressed by the surrounding good solder joints in a daisy-chain. In the open stage, a complete crack has occurred and the gap of the crack is large. Partial cracks are difficult to be detected by the electrical continuity measurement method due to limited resolution of commercial equipment. The duration of the crack stage depends on the severity of the test conditions.

It is recommended that the control-chart based method be used as failure criterion because it not only monitors the average of resistance, but also monitors the dispersion of resistance in each thermal cycle over time. 4 to 6 readings are suggested to be collected per thermal cycle. In addition to monitoring the resistance value, one could conclude that an interconnection may have failed if the range of resistance is significant larger than the theoretical range in a thermal fatigue reliability study. Monitoring the dispersion of resistance over time gives another way to detect failure of solder joints.

Acknowledgements
The author wants to thank Erin Kimura and Briana Fredericks for analyzing the reliability data. Thanks also go to Greg Henshall, Michael Fehrenbach, Chrys Shea, Ranjit Pandher, Ken Hubbard, Girish Wable, Gnyaneshwar Ramakrishna, Quyen Chu, and Ahmer Syed for sharing over 3.5 Gb resistance measurement data of the low-silver BGA project; to Reza Ghaffarian for reviewing this manuscript and providing valuable comments.

References

[1] J. H. Constable and C. Lizzul (1995), "An Investigation of Solder Joint Fatigue Using Electrical Resistance Spectroscopy," *IEEE Transactions on Components, Packaging, and Manufacturing Technology*, Part A, Vol. 18, No. 1, March 1995, pp. 142 – 152.

[2] P. Lall, R. Lowe, and K. Goebel (2009), "Resistance Spectroscopy-based Condition Monitoring for Prognostication of High Reliability Electronics Under Shock-Impact," Proceedings of IEEE Electronics Components and Technology Conference, pp. 1245 – 1255.

[3] J. Pan and J. Silk (2011), "A Study of Solder Joint Failure Criteria," Proceedings of 44th IMAPS International Symposium on Microelectronics, Long Beach, CA, 2011.

[4] I. Gershman and J. B. Bernstein, "Solder-joint Quantitative Crack Analysis – Ohmic Resistance Approach," *IEEE Transactions on Components, Packaging, and Manufacturing Technology*, Vol. 2, No. 5, May 2012, pp. 748 – 755.

[5] E. Kimura and J. Pan (2012), "Reliability Analysis of Low-Ag BGA Solder Joints Using Four Failure Criteria," Proceedings of 45th IMAPS International Symposium on Microelectronics, San Diego, CA, 2012.

[6] B. Fredericks (2013), "Reliability Analysis of Low-Silver BGA Spheres Comparing Failure Detection Criteria," Senior Project, California Polytechnic State University, San Luis Obispo, California.

[7] E. Kimura (2012), "Reliability Analysis of Low-Silver BGA Solder Joints Using Four Failure Criteria," Master Thesis, California Polytechnic State University, San Luis Obispo, California.

[8] G. Henshall, J. Bath, S. Sethuraman, D. Geiger, A. Syed, M.J. Lee, K. Newman, L. Hu, D. H. Kim, W. Xie, W. Eagar and J. Waldvogel, "Comparison of Thermal Fatigue Performance of SAC105 (Sn-1.0Ag-0.5Cu), Sn- 3.5Ag, and SAC305 (Sn-3.0Ag-0.5Cu) BGA Components with SAC305 Solder Paste," Proceedings of IPC APEX 2009.

[9] Montgomery, Douglas C. *Introduction to Statistical Quality Control*. New York: Wiley, 1985.

[10] G. Henshall, C. Shea, R. Pandher, A. Syed, Q. Chu, N. Tokotch, L. Escuro, M. Lapitan, G. Ta, A. Babasa, G. Wable, "Low-Silver BGA Assembly, Phase I – Reflow Considerations and Joint Homogeneity Reliability Assessment Initial Report," Proceedings of APEX, Las Vegas, NV, 2008.

[11] G. Henshall, M. Fehrenbach, C. Shea, Q. Chu, G. Wable, R. Pandher, K. Hubbard, G. Ramakrishna, A. Syed, "Low-Silver BGA Assembly, Phase II – Reliability Assessment. Sixth Report: Thermal Cycling Results for Unmixed Joints," SMTA International Conference Proceedings, 2010.

[12] G. Henshall, M. Fehrenbach, C. Shea, Q. Chu, G. Wable, R. Pandher, K. Hubbard, G. Ramakrishna, A. Syed, "Low-Silver BGA Assembly, Phase II – Reliability Assessment. Seventh Report: Mixed Metallurgy Solder Joint Thermal Cycling Results," Proceedings of IPC APEX, 2011.

[13] IPC-9701A (2006), "Performance Test Methods and Qualification Requirements for Surface Mount Solder Attachments," Association Connecting Electronics Industries.

[14] JESD22-B111 (2003), "Board Level Drop Test Method of Components for Handheld Electronic Products," JEDEC.

[15] IPC/JEDEC-9702 (2004), "Monotonic Bend Characterization of Board-Level Interconnects," IPC and JEDEC.

[16] D. C. Montgomery (2013), Introduction to Statistical Quality Control, 7th ed., Wiley.

[17] D. Besterfield (2009), Quality Control, 7th ed., Pearson Prentice Hall.

[18] H. Qi, N. M. Vichare, M. H. Azarian, and M. Pecht (2008), "Analysis of Solder Joint Failure Criteria and Measurement Techniques in the Qualification of Electronic Products," *IEEE Transactions on Component and Packaging Technologies*, Vol. 31, No. 2, June 2008, pp. 469- 477.

[19] Z. P. Wang, Y. M. Tan, and K.M. Chua (1999), "Board Level Reliability Assessment of Chip Scale Packages," *Microelectronics Reliability*, Vol. 39, No. 9, pp. 1351-1356.

[20] F. X. Che and J. H.L. Pang (2009), "Vibration Reliability Test and Finite Element Analysis for Flip Chip Solder Joints," *Microelectronics Reliability*, Vol. 49, No. 7, pp. 754-760.

[21] Q.J. Yang, H.L.J. Pang, Z.P. Wang, G.H. Lim, F.F. Yap, R.M. Lin (2000), "Vibration Reliability Characterization of PBGA Assemblies," Microelectronics Reliability, Vo. 40, pp. 1097–1107.

[22] Y.B. Kim, H. Noguchi, M. Amagai (2006), "Vibration Fatigue Reliability of BGA-IC Package with Pb-free Solder and Pb–Sn Solder," *Microelectronics Reliability*, Vol. 46, pp. 459–466.

[23] S.F. Wong, P. Malatkar, C. Rick, V. Kulkarni, I. Chin (2007), "Vibration Testing and Analysis of Ball Grid Array Package Solder Joints," Proceedings of 57th IEEE Electronic Components and Technology Conference, pp. 373−380.

[24] H. Qi, G. Plaza, S. Ganesan, M. Osterman, M. Pecht (2007), "Reliability Assessment on Insertion Mount Assembly under Vibration Conditions," Proceedings of 57th IEEE Electronic Components and Technology Conference, pp. 407−414.

[25] A. Perkins, S.K. Sitaraman (2008), "A Study into the Sequencing of Thermal Cycling and Vibration Tests," Proceedings of 58th IEEE Electronic Components and Technology Conference, pp. 584−592.

[26] F.X. Che and J. H.L. Pang (2013), "Fatigue Reliability Analysis of Sn-Ag-Cu Solder Joints Subject to Thermal Cycling," *IEEE Transactions on Device and Materials Reliability*, Vol. 13, No. 1, pp. 36-49.

[27] J. H. Lau, N. Hoo, R. Horsley, J. Smetana, D. Shangguan, D. Dauksher, D. Love, I. Menis, and B. Sullivan (2004), "Reliability Testing and Data Analysis of Lead-Free Solder Joints for High-density Packages," *Soldering & Surface Mount Technology*, Vol. 16, No. 2, 2004, pp. 46-68.

[28] M. Farooq, L. Goldmann, G. Martin, C. Goldsmith, C. Bergeron (2003), "Thermo-Mechanical Fatigue Reliability of Pb-Free Ceramic Ball Grid Arrays: Experimental Data and Lifetime Prediction Modeling," Proceedings of the 2003 IEEE Electronic Components and Technology Conference, pp. 827-831.

[29] J.C. Suhling, H.S. Gale, R.W. Johnson, M.N. Islam, T. Shete, P. Lall, M.J. Bozack, J.L. Evans, P. Seto, T. Gupta, and J.R. Thompson (2004), "Thermal Cycling Reliability of Lead-Free Chip Resistor Solder Joints," Soldering & Surface Mount Technology, Vol. 16, No. 2, pp. 77-87.

[30] W. Xie, T.K. Lee, K.C. Liu, and J. Xue (2010), "Pb-free Solder Joint Reliability of Fine Pitch Chip-Scale Package," Proceedings of the 2010 IEEE Electronic Components and Technology Conference, pp. 1587-1590.

[31] W.C. M. Filho, M. Brizoux, H. Fremont, and Y. Danto (2006), "Improved Physical Understanding of Intermittent Failure in Continuous Monitoring Method," *Microelectronics Reliability*, Vol. 46, pp. 1886-1891.

[32] F. Stepniak (2002), "Failure Criteria of Flip Chip Joints During Accelerated Testing," *Microelectronics Reliability*, Vol. 42, pp. 1921-1930.